Substrate Specificity Engineering of β-Mannosidase and β-Glucosidase from *Pyrococcus* by Exchange of Unique Active Site Residues†

Thijs Kaper,‡ Hester H. van Heusden,‡ Bert van Loo,‡ Andrea Vasella,§ John van der Oost,*,‡ and Willem M. de Vos‡

Laboratory of Microbiology, Department of Agrotechnology and Food Sciences, Wageningen University, H. van Suchtelenweg 4, NL-6703 CT, Wageningen, The Netherlands, and Laboratorium für Organische Chemie, ETH-Zentrum, Universitätstrasse 16, CH-8092 Zürich, Switzerland

Received October 16, 2001; Revised Manuscript Received February 4, 2002

ABSTRACT: A β-mannosidase gene (PH0501) was identified in the *Pyrococcus horikoshii* genome and cloned and expressed in *E. coli.* The purified enzyme (BglB) was most specific for the hydrolysis of *p*-nitrophenyl-β-D-mannopyranoside (pNP-Man) (K_m: 0.44 mM) with a low turnover rate (k_{cat}: 4.3 s^{-1}). The β-mannosidase has been classified as a member of family 1 of glycoside hydrolases. Sequence alignments and homology modeling showed an apparent conservation of its active site region with, remarkably, two unique active site residues, Gln77 and Asp206. These residues are an arginine and asparagine residue in all other known family 1 enzymes, which interact with the catalytic nucleophile and equatorial C2-hydroxyl group of substrates, respectively. The unique residues of *P. horikoshii* BglB were introduced in the highly active β-glucosidase CelB of *Pyrococcus furiosus* and vice versa, yielding two single and one double mutant for each enzyme. In CelB, both substitutions R77Q and N206D increased the specificity for mannosides and reduced hydrolysis rates 10-fold. In contrast, BglB D206N showed 10-fold increased hydrolysis rates and 35-fold increased affinity for the hydrolysis of glucosides. In combination with inhibitor studies, it was concluded that the substituted residues participate in the ground-state binding of substrates with an equatorial C2-hydroxyl group, but contribute most to transition-state stabilization. The unique activity profile of BglB seems to be caused by an altered interaction between the enzyme and C2-hydroxyl of the substrate and a specifically increased affinity for mannose that results from Asp206.

Family 1 glycosidases are found in all domains of life and have been classified as β-glucosidases, β-galactosidases, 6-phospho-β-glycosidases, lactase-phlorizin hydrolases, β-mannosidases, and myrosinases (*1*). While many members of this family have been demonstrated to be involved in energy supply or cell defense (*2*−*6*), not all characterized enzymes have clearly established metabolic roles (*7*). Family 1 enzymes have been shown to hydrolyze their substrates via a general acid/base-catalyzed mechanism with overall retention of the configuration at the C1 atom of the nonreducing sugar residue (*8, 9*). In this reaction, a covalent substrate−enzyme intermediate is formed, which has been trapped, allowing establishment of 3-D enzyme structures (*10*−*13*). The transition state in the retaining hydrolysis is generally believed to have a substantial oxycarbenium-cation-like character, as supported by the high sensitivity of family 1 glycosidases for inhibition by glycoside derivatives with a trigonal geometry at the anomeric carbon atom, such as glucono-lactones (*8, 9, 14*). Two glutamate residues are essential for the hydrolysis (*15*−*17*). Their pK_a-value is tightly regulated and, in analogy to family 11 xylanases, presumed to cycle during catalysis (*18*). Hydrogen bonds between the enzyme and substrate are crucial in the hydrolysis reaction, and the interaction with the C2-hydroxyl group of the glycoside contributes most to the stabilization of the transition state (*19, 20*). All family 1 glycoside hydrolases of which the 3-D structure has been determined revealed a $(\beta/\alpha)_8$-barrel as fold, although different quatenary organization forms have been observed, ranging from monomeric to octameric (*10, 21*−*28*). The enzyme−substrate interactions have been evaluated from enzymes that have been cocrystallized with ligands (*23, 28, 29*). Nine residues in the active site pocket have been found to interact directly with the substrate, and appear to be highly conserved throughout family 1 enzymes (*23*). Only the 6-phospho-β-glycosidases make up a separate group, since they have developed a phosphate binding site that enables the hydrolysis of 6-phospho-glycosides (*26, 29*).

The β-glucosidase CelB[1] of the hyperthemophilic archaeon *Pyrococcus furiosus* represents the most thermostable family 1 enzyme described to date (*15, 30*). The enzyme is active

† This research has been supported by Contract FAIR CT96-1048 of the European Union.

* To whom correspondence should be addressed. Tel: 31-317-483108, fax: 31-317-483829, email: john.vanderoost@algemeen.micr.wau.nl.

‡ Wageningen University.

§ ETH-Zentrum.

[1] Abbreviations: CelB, *P. furiosus* β-glucosidase CelB; BglB, *P. horikoshii* β-mannosidase BglB; pNP-Glc, *p*-nitrophenyl-β-D-glucopyranoside; pNP-Gal, *p*-nitrophenyl-β-D-galactopyranoside; pNP-Man, *p*-nitrophenyl-β-D-mannopyranoside; X-glu, 5-bromo-4-chloro-3-indolyl-β-D-glucopyranoside; PheImGlc, (5*R*,6*R*,7*S*,8*S*)-5-(hydroxymethyl)-2-phenyl-5,6,7,8-tetrahydroimidazol[1,2-*a*]pyridine-6,7,8-triol.

10.1021/bi011935a CCC: $22.00
Published on Web 03/03/2002

as a tetramer and displays a high hydrolytic activity with a half-life of 85 h at 100 °C (*30*). In agreement with its involvement in the degradation of glucans (*4*, *30*, *31*), CelB displays the highest hydrolytic efficiency on glucosides and fucosides, but the enzyme is also capable of hydrolyzing galactosides and, to a lower extent, mannosides as well (*30*, *32*). The mechanism of glycoside hydrolysis by *P. furiosus* CelB at extremely high temperatures was found to be similar to that of the related mesophilic β-glucosidase from *Agrobacterium faecalis* (*32*). CelB has been crystallized, and a structural model of the enzyme was constructed based on a 3.3 Å resolution X-ray diffraction data set (*26*). Analysis of CelB's active site revealed a high structural similarity to that of the previously determined 6-phospho-β-galactosidase LacG of *Lactococcus lactis* (*26*).

In the genome sequence of the hyperthermophilic archaeon *Pyrococcus horikoshii*, two open reading frames have been annotated as family 1 glycoside hydrolases (*33*, *34*). PH0366 encodes a membrane-associated protein with high efficiency for the hydrolysis of long-chain alkyl-glycosides (*35*). The hydrolase encoded by PH0501 has been annotated as a β-mannosidase (*33*) based on amino acid homology with the characterized β-mannosidase BmnA from *P. furiosus* (*7*). However, this has not yet been verified experimentally.

This study describes the cloning and expression of PH0501, and the characterization of its gene product, the β-mannosidase BglB. This new thermostable member of glycoside hydrolase family 1 has a low hydrolytic activity. Multiple sequence alignment and 3-D modeling reveal that BglB represents a new subgroup of family 1 glycoside hydrolases, characterized by two unique active site residues. Their role was studied by substituting them for the corresponding residues of the well-characterized β-glucosidase CelB of *P. furiosus* by site-directed mutagenesis, and vice versa. The catalytic activity of the mutant enzymes has been compared to wild-type variants, and the effects of the substitutions on substrate binding and catalysis are discussed in detail.

MATERIALS AND METHODS

Strains, Plasmids, and Chemicals. Escherichia coli BL21(DE3) was used as a host for the cloning and production of wild-type and mutant enzymes. All genes were cloned in the expression vector pET9d (Novagen). Expression plasmid pLUW511 was used for the production of wild-type CelB, as described (*36*). All chemicals were of analytical grade. The chromogenic substrates *p*-nitrophenyl-β-D-glucopyranoside (pNP-Glc), *p*-nitrophenyl-β-D-galactopyranoside (pNP-Gal), and *p*-nitrophenyl-β-D-mannopyranoside (pNP-Man) were obtained from Sigma. 5-Bromo-4-chloro-3-indolyl-β-D-glucopyranoside (X-glu) was purchased from Biosynth (Staad, Switzerland). The thermostable transition-state analogue (5*R*,6*R*,7*S*,8*S*)-5-(hydroxymethyl)-2-phenyl-5,6,7,8-tetrahydroimidazol[1,2-*a*]pyridine-6,7,8-triol (PheImGlc) was synthesized as described (*14*). Chromosomal DNA of *P. horikoshii* OT3 was kindly provided by Ir. C. Verhees (Wageningen University, Wageningen, The Netherlands).

Cloning of the P. horikoshii bglB Gene. The open reading frame PH0501 coding for BglB (GenBank AP000002) was identified by a BLAST search of the *P. horikoshii* OT3 genome sequence using the CelB amino acid sequence. Based on the presence of a putative Shine−Dalgarno sequence, the translation start site of the *bglB* gene was predicted, which resulted in a protein that corresponded in size and composition to other family 1 enzymes. The gene was amplified by PCR using the 5′-oligonucleotide BG461 and the 3′-oligonucleotide BG462. BG461 (5′-gcgcgccATGgcaAAGTTT-TACTGGGGC GTCGTT-3′ (*bglB* sequence in capitals) introduced an alanine residue following the initiator methionine in order to create a *Nco*I site (underlined) that allowed a translational fusion of *bglB* to the T7 promoter of pET9d. BG462 (5′-gcgcgcgctcagcTTATTTTCTTCCAGG-TAGTTTCAT-3′) introduced a *Blp*I site (underlined) after the stop codon of *bglB*. The alanine at position 2 will be referred to as Ala2, which results in an identical residue numbering for a large part of both proteins. PCR reactions (50 μL) contained 2.5 units of *Pfu* DNA polymerase (Stratagene) in the supplied buffer, 0.2 mM of each dNTP, 20 ng of chromosomal *P. horikoshii* DNA, and 10 pmol of each primer. The reactions were subjected to a denaturation step of 5 min at 95 °C followed by 35 repeats of 1 min at 95 °C, 45 s at 50 °C, and 90 s at 72 °C, followed by 5 min at 72 °C. PCR products were recuperated in 2 mM Tris-HCl, pH 8.0, after purification using a PCR purification kit (QIAgen). The PCR product and pET9d vector were digested by *Nco*I and *Blp*I, isolated from agarose gel using the QiaexII gel extraction kit (QIAgen), and ligated together. *E. coli* BL21(DE3) was transformed with the ligation mix by electroporation and plated on selective TY plates containing X-glu. Colonies expressing functional β-glycosidase activity were selected by their blue phenotype, since X-glu cannot be hydrolyzed by *E. coli* LacZ β-galactosidase. The nucleotide sequence of the *bglB* gene in plasmids from positive colonies was verified by DNA sequence analysis using the Thermosequenase cycle sequencing kit (Amersham-Pharmacia-Biotech) with infrared dye-labeled primers. This provided the same sequence as deposited in the database (*33*). Reactions were analyzed on a LiCor 4000L automated sequencer (data not shown). The resulting construct was denoted pLUW527.

Homology Modeling. The BglB primary sequence was submitted to the Swiss model homology server (*37*). The structures of the β-glycosidases from *Sulfolobus solfataricus* (LacS, PDB: 1GOW) and *Thermosphaera aggregans* (Bgly, PDB: 1QVB) and the 6-phospho-β-galactosidase LacG from *Lactococcus lactis* (PDB: 2PBG) were used as templates in the modeling procedure. The quality of the model was verified using the programs Procheck (*38*) and Prosa (*39*). A galactose molecule was modeled in the active site of BglB by superposition of the active sites of BglB and *L. lactis* LacG, crystallized with the ligand in the active site (*26*, *29*).

Construction of Mutants. Mutations were introduced in *celB* and *bglB* using *Pfu* DNA polymerase using the PCR-based overlap extension method (*40*). For each mutation, a sense/antisense primer pair was designed. R77Q was introduced in CelB by BG652 (ATGGATTGTATA**CA**AGG-TGGCATTGA)/BG653 (TCAATGCCACCT**TG**TATAC-AATCCAT) (*Acc*I). BG530 (5′-GACATGTGG**TCG**AC-AATGGACGAACCAAAC-3′)/BG531 (5′-GTTTGGTTCGT-**C**CATTGT**CGA**CCACATGTC-3′) (*Sal*I) introduced N206D in CelB (introduced mutations in boldface type, introduced restriction sites underlined, and restriction enzymes in parentheses). BG654 (TTGAATGCTTATC**G**ATTAACG-

ATAG)/BG655 (CTATCGTTAATCGATAAGCATTCAA) (*Cla*I) introduced Q77R in BglB. BG528 (5′-GATTACTG-GTC**G**ACATTT**A**ATGAACCAATG-3′)/BG529 (5′-CATTG-GTTCAT**T**AAATGT**C**GACCAGTAATC-3′) (*Sal*I) resulted in D206N in BglB. These primers were used in combination with BG238/BG239 in the case of *celB* (*36*) and with BG461/462 in the case of *bglB* (see above). Mutated *bglB* and *celB* genes were cloned and isolated as described above. Plasmid pLUW511 (CelB wild-type) was used for the construction of pLUW524 (CelB R77Q) and pLUW525 (CelB N206D). Plasmid pLUW525 served as template for the construction of pLUW526 (CelB R77Q/N206). Likewise, pLUW527 (wild-type BglB) was used to construct pLUW528 (BglB Q77R) and pLUW529 (BglB D206N). Plasmid pLUW533 (BglB Q77R/D206N) was constructed using pLUW529. Introduced mutations were confirmed by restriction analysis and DNA sequence analysis (see above).

Enzyme Production and Purification. Enzymes were produced and purified essentially as described before (*26*). The cell-free extracts of wild-type and mutant BglB-producing BL21(DE3) strains were subjected to an extra centrifugation step of 10 min at 6000 rpm followed by a heat incubation of 40 min at 80 °C. Heat-stable cell-free extracts were applied on an anion exchange column (Q-Sepharose, Amersham-Pharmacia-Biotech) equilibrated with 20 mM Tris-HCl (pH 8.0) and eluted with a linear NaCl gradient (0−1.0 M). Pure protein was obtained after applying the pooled active fractions on a hydrophobic interaction column (phenyl-Sepharose, Amersham-Pharmacia-Biotech), equilibrated with 20 mM Tris-HCl (pH 8.0) with 1 M $(NH_4)_2SO_4$ followed by elution during a linear decreasing $(NH_4)_2SO_4$ gradient (1.0−0 M). Active fractions were pure as judged by SDS−PAGE analysis, and pooled fractions were dialyzed against 20 mM NaP_i (pH 7.5). The protein solutions were stored at 4 °C and contained 0.02% NaN_3 to prevent microbial growth. Protein concentrations were measured at 280 nm according to Gill and Hippel (*41*), in which calculated ϵ_{280}-values of 128 280 and 120 740 M^{-1} cm^{-1} were used for CelB and BglB, respectively.

Molecular Weight Determination by Gel Filtration. Samples of 100 μg of purified BglB and CelB were loaded on a Superdex 200 HR16/60 column (Amersham-Parmacia-Biotech) equilibrated with 100 mM NaCl in 20 mM Tris-HCl (pH 8.0) and eluted at a rate of 0.5 mL/min using an Äkta FPLC (Amersham-Pharmacia-Biotech). Besides the CelB protein with a previously determined size of 230 kDa (*30*), blue dextran (2000 kDa), thyroglobin (669 kDa), ferritin (440 kDa), catalase (232 kDa), chymotrypsin (25 kDa), and ribonuclease (13.7 kDa) were used as standard mass markers.

Kinetic Stability. Kinetic stability was measured as described (*42*). Aliquots of wild-type BglB and CelB were diluted to 0.05 mg/mL in 150 mM sodium citrate (pH 5.0). Samples of 100 μL were dispensed in glass vials closed with a Teflon cap and submersed in silicon oil of 106 °C. At regular intervals, vials were removed from the oil and immediately chilled on ice. Residual activity was determined using a routine activity assay (*42*). Half-lives of inactivation were calculated from data fits according to first-order kinetics using the nonlinear regression program Tablecurve 2D (Jandel Scientific).

Differential Scanning Calorimetry. Protein solutions of wild-type CelB and BglB were dialyzed extensively against 20 mM Na P_i (pH 7.5) and diluted to 4.6 and 4.4 μM in dialysis buffer, respectively. After 10 min degassing and equilibration, samples were analyzed in a VP-DSC differential scanning micro-calorimeter (MicroCal) between 50 and 125 °C at 0.5 °C/min against the dialysis buffer. Enzyme scans were corrected using a buffer−buffer baseline.

Kinetic Analyses. The optimal pH for hydrolysis and kinetic constants by wild-type and mutant enzymes at 90 °C were determined as described in earlier studies (*26*). The optimal pH for hydrolysis was determined for 15 mM pNP-Glc. To determine the kinetic parameters of the enzyme variants at their respective optimal pH at 90 °C, enzyme-catalyzed hydrolysis was determined at 10−15 different concentrations of pNP-Glc (0−20 mM), pNP-Gal (0−25 mM), and pNP-Man (0−12 mM) bracketing the K_m, when possible. Liberated pNP was measured at 405 nm using a U-2010 spectrophotometer (Hitachi) equipped with a temperature controller. Specific absorption coefficients of pNP were determined at 90 °C: $\epsilon_{405,pH4.8}$: 556 M^{-1} cm^{-1}, $\epsilon_{405,pH5.0}$: 905 M^{-1} cm^{-1}, $\epsilon_{405,pH5.2}$: 1200 M^{-1} cm^{-1}. Data were fitted according to Michaelis−Menten kinetics using the nonlinear regression program Tablecurve 2D (Jandel Scientific). The turnover number, k_{cat}, has been defined as the amount of substrate molecules converted per second per active site in which molecular masses of 54 664 and 56 467 Da were used for subunits of wild-type CelB and wild-type BglB, respectively. The K_i-value for the inhibition by PheImGlc was first estimated by measuring the enzyme-catalyzed hydrolysis at a fixed concentration of pNP-Glc close to the K_m-value in the presence of varying inhibitor concentrations and plotting the data in a Dixon plot. Activities of enzyme-catalyzed hydrolysis were determined at five different substrate concentrations, bracketing the K_m, and seven different inhibitor concentrations, around the estimated K_i-value. The final K_i was calculated from fitting the data using the nonlinear regression program Tablecurve 3D (Jandel Scientific) using a formula for competitive inhibition (*43*).

RESULTS AND DISCUSSION

Primary Sequence Analysis of P. horikoshii BglB. Open reading frame PH0501 of *P. horikoshii* is predicted to code for a 483 amino acid protein with a calculated size of 56 457 Da, designated here as BglB, and has been classified as a member of family 1 of glycoside hydrolases in the CAZy database (*1*). It shows the highest protein sequence identity (>70%) and clusters together in a phylogenetic tree with putative BglB-like proteins from other species from the order of Thermococcales (Figure 1A). The well-characterized *P. furiosus* β-glucosidase CelB (37% amino acid identity) (*15*) and *S. solfataricus* β-glycosidase LacS (38%) (*44*) are relatively distantly related to BglB. Since crystal structures of CelB and LacS and the *Thermosphaera aggregans* β-glycosidase Bgly (40%) are available (*24*−*26*), these enzymes can be used for structural interpretation of the BglB sequence as well as for the construction of a 3-D model. The β-mannosidase BmnA (56%) from *P. furiosus* is the characterized glycosidase most closely related to *P. horikoshii* BglB (*7*).

A remarkable characteristic of family 1 glycoside hydrolases is the high degree of conservation of the amino acid residues that are involved in catalysis and substrate binding.

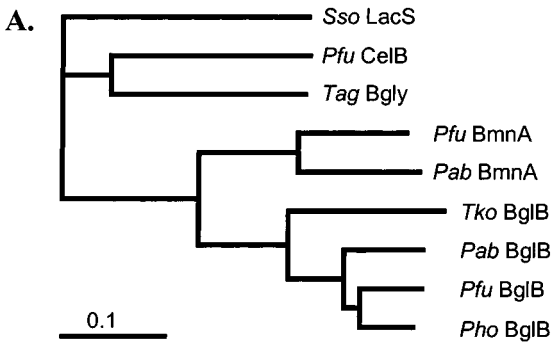

B.

```
Pho BglB   40 : KNDLVSGDLPEEGINNYELYEIDHRLAKELGLNAYQLTIEWSRIF :  85
Pfu BglB   40 : KNELVSGDLPEEGINNYDLYEIDHRLAKDLGLNAYQLTIEWSRIF :  85
Pab BglB   40 : KNELVSGDLPEEGINNYELYEIDHRLAKELGLNAYQLTIEWSRIF :  85
Tko BglB   41 : KNDLVSGHLPEDGINNYGLYEIDHQLAKDMGLNAYQITVEWSRIF :  86
Pfu BmnA   43 : EKGLVSGDLPEEGINNYELYEKDHEIARKLGLNAYRIGIEWSRIF :  88
Pab BmnA   43 : EKGLVSGDLPEDGINSYELYEVDHNLAKDLGLNMYRIGIEWSRIF :  88
Pfu CelB   41 : ASGLVSGDLPENGPAYWHLYKQDHDIAEKLGMDCIRGGIEWARIF :  86
Tag Bgly   42 : AAGLVSGDFPENGPGYWNLNQNDHDLAEKLGVNTIRVGVEWSRIF :  87
Sso LacS   43 : AAGLVSGDLPENGPGYWGNYKTFHDNAQKMGLKIARLNVEWSRIF :  88
                                                  ⇑
                                                  1

Pho BglB  174 : VDERTIIEFAKYAAYVAWKFDNYVDYWSTFDEPMVTAELGYLAPY : 219
Pfu BglB  174 : VDEKTIVEFVKYVAYVAWKFDQYVDYWATFDEPMVTVELGYLAPY : 219
Pab BglB  174 : VDERAIVEFSKFAAYVAWKFDKYVDFWATFDEPMVTAELGYLAPY : 219
Tko BglB  175 : VDERAILEFAKFAAFVAWKRWDLVDYWATFDEPMVTVELGYLAPY : 220
Pfu BmnA  178 : VNPRTVIEFAKYAAYIAYKFGDIVDMWSTFNEPMVVVELGYLAPY : 223
Pab BmnA  178 : INKRTVIEFAKFAAYIAYKFGDIVDMWSTFNEPMVVVELGYLAPY : 223
Pfu CelB  175 : LDEKTVVEFVKFAAFVAYHLDDLVDMWSTMNEPNVVYNQGYINLR : 220
Tag Bgly  176 : LNEESVVEFAKYAAYIAWKMGELPVMWSTMNEPNVVYEQGYMFVK : 221
Sso LacS  174 : LSTRTVYEFARFSAYIAWKFDDLVDEYSTMNEPNVVGGLGYVGVK : 219
                                            ⇑#
                                            2

Pho BglB  463 : RIPRRRSVEIYKKIVM-EGIE------------------------ : 483
Pfu BglB  463 : RIPRRKSVETYKMIVA-EGIE------------------------ : 483
Pab BglB  463 : RIPRRKSVETYKKVVK-EGIE------------------------ : 483
Tko BglB  463 : RIPRPRSVETYKKIVR-EGLP------------------------ : 483
Pfu BmnA  478 : RIPREKSVSIFREIVANNGVTKKIEEEL---LRGM---------- : 510
Pab BmnA  479 : RKPRKRSVEVFSRIIS-EGTTKGLQDEFRLKVRGERYENDSG--- : 520
Pfu CelB  437 : RYLR-PSALVFREIATQKEIPEELAHLADLKFVTRK--------- : 472
Tag Bgly  451 : RYLR-PSALVFREIATHNGIPDELQHLTLIQ-------------- : 481
Sso LacS  452 : LYWR-PSALVYREIATNGAITDEIEHLNSVPPVKPLRH------- : 489
```

FIGURE 1: (A) Phylogenetic tree of thermostable (putative) family 1 glycoside hydrolases: Pho_BglB: *P. horikoshii* β-mannosidase (GenBank AP000002), Pab_BglB: *P. abyssi* putative β-mannosidase BglB (AJ248288), Pfu_BglB: *P. furiosus* putative β-mannosidase BglB (*P. furiosus* genome ORF Pf_368506), Tko_BglB: *Thermococcus kodakaraensis* putative β-mannosidase BglB (GenBank AB028601), Pfu_BmnA: *P. furiosus* β-mannosidase BmnA (U60214), Pab_BmnA: *P. abyssi* putative β-mannosidase BmnA (AJ248285), Pfu_CelB: *P. furiosus* β-glucosidase CelB (AF013169), Tag_Bgly: *T. aggregans* β-glycosidase (AF053078), Sso-LacS: *S. solfataricus* β-glycosidase LacS (M34696). Alignment and tree were generated in ClustalX (*54*), and the tree was visualized using Treeview (*55*). (B) Alignment of partial protein sequences of the above-mentioned thermostable family 1 glycoside hydrolases; "1" and "2" indicate positions of unique glutamine and aspartic acid residues in BglB, respectively, and "#" indicates active site catalytic acid/base residue.

Surprisingly, all BglB sequences were characterized by two active site residues which are different from those present in other family 1 glycoside hydrolases. In *P. horikoshii* BglB, these residues are the glutamine at position 77 and the aspartic acid at position 206 (Figure 1B, indicated by 1 and 2). In all other family 1 enzymes, these residues are an arginine and an asparagine, respectively. This identifies the BglB proteins as a new subfamily of family 1 glycoside hydrolases.

Characterization of P. horikoshii BglB. P. horikoshii ORF PHO501 was overexpressed in *E. coli* BL21(DE3). Although the majority of the protein was expressed as nonsoluble, inactive inclusion bodies, a small fraction (~5%) was soluble and active and could be purified to homogeneity (Figure 2, lanes 1, 2). Attempts to improve the functional expression of the *bglB* gene by varying the addition and amount of IPTG induction, or growth temperature, did not result in increased production yields (data not shown). The biochemical properties of the purified BglB were compared to those of *P. furiosus* β-glucosidase CelB. The native form and thermostability of BglB and CelB were studied by boiling of protein samples. When BglB was not boiled, it was found to migrate as a complex of high molecular mass on a SDS−PAGE gel (Figure 2, lane 1, A). After 10 min boiling in SDS-sample buffer, virtually all BglB has been denatured, although a small portion is still present as a multimer with an apparent size of about 160 kDa (Figure 2, lane 2, B). On the other hand, the CelB protein is mainly present in what is generally accepted as the tetrameric form (*29*), which appears as a protein band of about 150 kDa (Figure 2, lane 3). When CelB is boiled for 10 min, only a fraction of the protein is fully denatured and appears at the position of the size of a single subunit (Figure 2, lane 4). The position of denatured monomeric BglB (Figure 2, C) correlates with the calculated

Table 1: Kinetic Parameters for the Hydrolysis of pNP-Glc, pNP-Gal, and pNP-Man and PheImGlc Inhibition of Wild-Type BglB and BglB Mutants at 90 °C in 0.1 M Sodium Citrate/0.1 M NaP_i[a]

enzyme	substrate	K_m (mM)	k_{cat} (s^{-1})	k_{cat}/K_m ($s^{-1}\,mM^{-1}$)	%	$K_{i,PheImGlc}$ (nM)
BglB wild-type	pNP-Glc	13.5 ± 3.3	34.4 ± 4.3	2.58	26	1.0×10^5
	pNP-Gal	7.3 ± 1.1	13.5 ± 1.0	1.9	20	
	pNP-Man	0.44 ± 0.10	4.2 ± 0.3	9.8	100	
BglB Q77R	pNP-Glc	16.2 ± 2.3	25.5 ± 2.2	1.6	100	1.1×10^5
	pNP-Gal	16.8 ± 2.9	14.2 ± 1.4	0.85	54	
	pNP-Man	1.1 ± 0.2	1.6 ± 0.1	1.4	91	
BglB D206N	pNP-Glc	0.30 ± 0.04	252 ± 9	870	100	14
	pNP-Gal	7.8 ± 1.0	571 ± 32	75.8	8.7	
	pNP-Man	3.2 ± 1.1	45.0 ± 5.0	14.7	1.7	
BglB Q77R/D206N	pNP-Glc	30.4 ± 3.5	439 ± 36	14.4	100.0	2.0×10^4
	pNP-Gal	36.1 ± 5.7	66.5 ± 7.3	1.8	13	
	pNP-Man	0.68 ± 0.4	6.8 ± 0.4	9.9	69	

[a] In the assays, between 0.48 and 1.1 μg of protein was used.

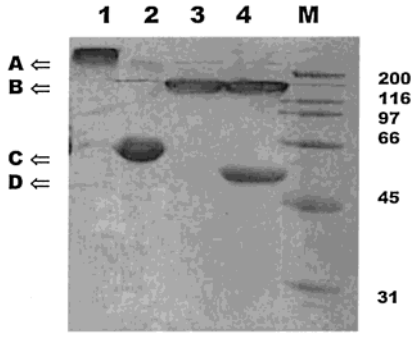

FIGURE 2: SDS−PAGE gel of purified BglB and CelB. Lanes 1 and 2 are BglB (15 μg); lanes 3 and 4 are CelB (21 μg). Before loading, lanes 1 and 3 were not incubated; lanes 2 and 4 were incubated for 10 min at 100 °C in SDS-sample buffer. M: BioRad broad range marker, sizes in kDa. Arrows indicate positions of BglB multimer complex (A), CelB tetramer (B), BglB monomer (C), and CelB monomer (D).

subunit size (56.5 kDa), which is slightly larger than that of monomeric CelB (52.1 kDa) (Figure 2, D). In gel filtration studies, the active form of BglB eluted at a position that corresponded to a molecular size of about 250 kDa. This suggests that the active form of BglB is a tetramer, as has been found for both the β-glucosidase CelB and the β-mannosidase BmnA of *P. furiosus*, the β-glycosidase LacS of *S. solfataricus*, and the β-glycosidase of *T. aggregans* (*7*, *25*, *45*, *46*).

The thermostability of BglB was compared to CelB by heat incubation at 102 °C. The half-life of activity of BglB was 27 min, while that of CelB was over 10 h at this temperature. For BglB and CelB, apparent melting temperatures of 100.7 and 106.0 °C were determined, respectively, which correlated with the determined half-lives at 102 °C. The lower stability of BglB can be partly explained by the relatively short C-terminus of BglB. The longer C-terminus of *S. solfataricus* LacS is involved in an intricate ion-pair network that bridges the four subunits at the center of the protein (*24*). A similar, though less extensive, interaction is postulated too for *P. furiosus* CelB, where the penultimate arginine residue is reaching toward an aspartic acid residue of an adjacent subunit to form a salt bridge (*47*). These interactions in LacS and CelB contribute to their stability (*47*, *48*). Such stabilizing interactions are ruled out for BglB, where the C-terminus is 16 residues shorter compared to *P. furiosus* CelB.

Optimal hydrolytic activity of BglB at 90 °C was observed at pH 4.75 (data not shown). The kinetic parameters of the enzyme for the hydrolysis of pNP-Glc, pNP-Gal, and pNP-Man were determined at 90 °C (Table 1). If *P. horikoshii* BglB can be taken as a representative, the members of this subfamily display very low hydrolytic activities, as compared to the related β-mannosidase BmnA and β-glucosidase CelB from *P. furiosus* (*7*, *30*, *42*) (Tables 1 and 2). Although BglB has the highest turnover rates for the hydrolysis of pNP-Glc and pNP-Gal, it should be classified as β-mannosidase, because it has the highest catalytic efficiency for the hydrolysis of pNP-Man.

3-D Structural Model of BglB and Active Site Topology. The 3-D model of BglB as obtained from the PDB homology server was analyzed with Procheck (*38*) and Prosa (*39*). The majority of the residues (96%) were located in the energetically most favorable or allowed regions of the Ramachandran plot of dihedral angles, with few in the generously allowed (2%) or disallowed (2%) regions. The *Z*-score of the *P. horikoshii* BglB model was −10.14, which makes it a reliable model (*49*). As expected from the modeling procedure, the overall structure of the BglB model shows a $(\beta/\alpha)_8$-barrel that resembles that of CelB to a high extent. An overlay of the active sites of BglB and CelB shows the conservation of the positions of the active site residues (Figure 3A). A galactose molecule modeled in the active site visualizes the position of the two unique active site residues Gln77 and Asp206 with respect to the catalytic glutamate residues and the substrate (Figure 3B). These residues are located close to the two catalytic glutamate residues, which act as a nucleophile (BglB Glu399, CelB Glu372) and a catalytic acid/base (both Glu207) in the hydrolysis reaction. The positions of backbone atoms of the unique glutamine 77 and aspartic acid 206 in BglB are identical to the corresponding residues of CelB (Figure 3B). Due to the shorter side chain, therefore, Gln77 is not able to reach into the active site of BglB as far as Arg77 in CelB. Arg77 presumably forms a salt bridge with the catalytic residue Glu372 in CelB, while in BglB there is no interaction possible between Gln77 and the corresponding catalytic residue Glu399. Asp206, the other unique active site residue, occupies the same space as its isosteric CelB counterpart Asn206. The corresponding residue of Asp206 in BglB has been found to interact with the hydroxyl group at carbon atom 2 of glucosides and galactosides in resolved crystal structures of other family 1

Table 2: Kinetic Parameters for the Hydrolysis of pNP-Glc, pNP-Gal, and pNP-Man and PheImGlc Inhibition of Wild-Type CelB and CelB Mutants at 90 °C in 0.1 M Sodium Citrate/0.1 M NaP_i[a]

enzyme	substrate	K_m (mM)	k_{cat} (s^{-1})	k_{cat}/K_m (s^{-1} mM^{-1})	%	$K_{i,PheImGlc}$ (nM)
CelB wt	pNP-Glc	0.19 ± 0.06	1140 ± 86	7337	100	6.5
	pNP-Gal	5.0 ± 0.25	2827 ± 46	561	7.6	
	pNP-Man	1.3 ± 0.1	65.9 ± 1.6	49.8	0.7	
CelB R77Q	pNP-Glc	13.8 ± 3.0	207 ± 25	14.9	100	97
	pNP-Gal	21.7 ± 3.0	69.2 ± 5.8	3.2	21	
	pNP-Man I	0.64 ± 0.12	1.22 ± 0.05	1.9	13	
	pNP-Man II	0.15 ± 0.04	0.85 ± 0.07	5.7	38	
CelB N206D	pNP-Glc	4.6 ± 0.06	116 ± 7	24.9	100	9.8×10^3
	pNP-Gal	15.7 ± 2.0	180 ± 13	11.5	46	
	pNP-Man	0.63 ± 0.07	1.97 ± 0.07	3.1	13	
CelBR77Q/N206D	pNP-Glc	13.9 ± 1.2	172 ± 8	12.3	100	2.7×10^3
	pNP-Gal	22.0 ± 2.6	29.2 ± 2.1	1.3	11	
	pNP-Man I	1.5 ± 0.2	1.9 ± 0.1	1.3	11	
	pNP-Man II	0.10 ± 0.01	1.02 ± 0.03	10.2	83	
CelB N206S[b]	pNP-Glc	12	309	26	100	
	pNP-Gal	200[c]	1090[c]	5.5	21	
	pNP-Man	4.7	15	3.2	12	

[a] In the assays, between 85 ng and 2.0 μg of protein was used. Mutants CelB R77Q and R77Q/N206D showed a biphasic behavior for the hydrolysis of pNP-Man (Figure 4) with separate kinetic parameters above (I) and below (II) 1 mM pNP-Man. [b] Values obtained from Lebbink et al. (*36*). [c] Estimated values, due to the limited solubility of pNP-Gal.

glycosidases with bound ligands in the active site (*23*, *29*). The almost identical position of BglB Asp206 to that of CelB Asn206 suggests that it is close enough for an interaction with the hydroxyl at position 2 of the galactose molecule (Figure 3B). Interestingly, this is the hydroxyl group which is axial in mannose and equatorial in glucose. However, the interactions of a mannoside with the enzyme can be expected to be different from those in Figure 3B. Upon binding in the active site, the sugar ring is likely to be distorted, as found previously in family 5 endo-β-glucosidase Cel5A of *Bacillus agaradhaerans* (*50*). This will bring the glycosidic oxygen atom of the mannoside in plane with catalytic acid Glu207, after which the glycosyl-enzyme intermediate is formed (*50*). The β-1,4-glucanase Cex from *Cellulomonas fimi* hydrolyzes β-glucosides by the retaining mechanism, like CelB. The C2-hydroxyl group of a covalently bound glucose residue in the −1 subsite in the active site of Cex has been found to have a strong interaction with the carbonyl oxygen of the carboxyl group of the nucleophilic glutamate (*13*). This interaction is highly stabilizing in hydrolysis, hence the reduction in activity of β-glycosidases upon removal of the equatorial C2-hydroxyl group of a glycosidic substrate (*19*, *51*). Due to the axial C2-hydroxyl, a mannose molecule is not capable of a similar interaction.

Production of Mutant Enzymes. To analyze the role of the unique residues in the BglB active site, their CelB counterparts were introduced in BglB and vice versa. This resulted in two sets of mutants. The first set consisted of BglB variants that possess one or two CelB residues in the active site, two single mutants (BglB Q77R and BglB D206N), and one double mutant (BglB Q77R/D206N). The second set was made up by three CelB counter-mutants, two single mutants (CelB R77Q and CelB N206D), and one double mutant (CelB R77Q/N206D). The enzymes were produced in *E. coli* BL21(DE3). The mutant enzymes resembled the corresponding wild-type enzymes in production and purification, indicating proper folding. Similar as for the wild-type protein, about 5% of the BglB mutants were present in the soluble fraction, and up to 2 mg of each BglB variant protein could be purified per liter of cell culture.

pH Optima of Mutant and Wild-Type Enzymes. The optimal pH for hydrolysis of pNP-Glc at 90 °C was determined (pH 3−8). It was found that both the wild-type and mutant BglB and CelB variants show optimal catalysis at pH 4.75−5.0 (data not shown). Above pH 5.0, however, the k_{cat} of BglB Q77R decreased more rapidly than that of the wild-type. In contrast, BglB D206N was relatively insensitive to a pH change above pH 5.0. The CelB mutants showed pH profiles identical to wild-type CelB. These findings are remarkable, since the known cases of removal or introduction of charges in the active site of CelB and other β-glycoside hydrolases have resulted in significant pH-shifts for optimal hydrolysis (*26*, *52*).

Kinetic Parameters of Mutant and Wild-Type Enzymes. The catalytic parameters of wild-type CelB and CelB mutants for the hydrolysis of pNP-Glc, pNP-Gal, and pNP-Man have been determined (Table 2). Wild-type CelB can be regarded as a β-glucosidase; it has the highest catalytic efficiency for the hydrolysis of pNP-Glc. However, the broad substrate specificity commonly found for family 1 enzymes was illustrated by CelB's considerable galactosidase activity and, although modest, mannosidase activity. When the unique residues of BglB were introduced in CelB, the hydrolyses of pNP-Glc and pNP-Gal were affected similarly: both the rate of hydrolysis and the substrate affinity decreased (Table 2). R77Q and N206D also reduced the turnover rate for pNP-Man in CelB (77- and 33-fold, respectively); however, the affinity for pNP-Man was increased (8- and 2-fold, respectively). When Asn206 was replaced by a shorter and uncharged serine, the affinity of CelB for all substrates decreased, although the increase in the K_m-value for the hydrolysis of mannosides was moderate compared to those for hydrolysis of gluco- or galactosides (*36*). The k_{cat} in this mutant, however, is less affected, compared to N206D (Table 2). CelB N206D has a higher affinity for all tested substrates than CelB N206S. This indicates the presence of an interaction between D206 and the substrate in CelB N206D. The drop in k_{cat} in this mutant, compared to N206S, suggests that the aspartic acid is dissociated during the catalysis cycle. It is this charge, however, that seems to result in an increased

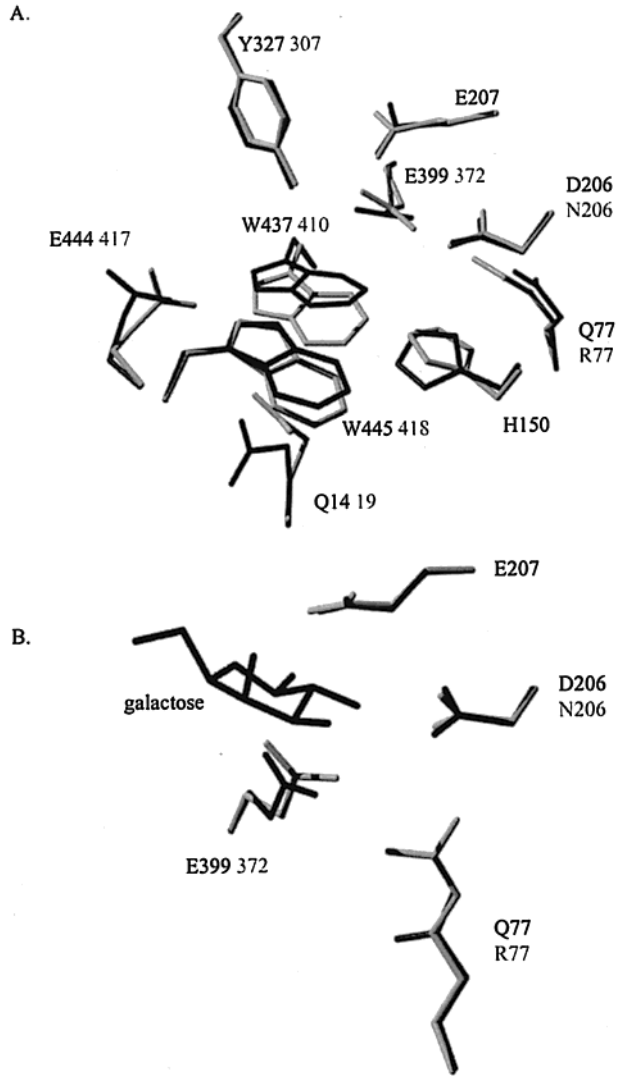

FIGURE 3: Superposition of the active site residues BglB (black) and CelB (gray; only residue numbers that differ from BglB have been indicated) (*26*) that align with substrate binding residues of *L. lactis* LacG (*29*) and *B. polymyxa* BglA (*23*) (A); close-up of unique BglB residues and catalytic glutamic acid residues (black) superimposed with corresponding CelB residues (gray) and a modeled galactose molecule (B). Images were made in PDBviewer (*56*) and visualized using Povwin (*57*).

affinity for mannosides. The combination of R77Q and N206D showed an additive effect and gave an enzyme with the combined activities of both separate mutants: the substrate affinity of R77Q combined with the slightly higher activity of N206D. This resulted in an increased efficiency for the hydrolysis of mannosides. The mutants containing the substitution R77Q were more efficient in the hydrolysis of pNP-Man, than of pNP-Gal. The Lineweaver−Burk plot for the hydrolysis of pNP-Man by these mutants was biphasic (Figure 4), which is an indication for oligosaccharide synthesis, as observed previously (*8*, *32*). Indeed, products corresponding in size to saccharide oligomers were detected by FPLC analysis in samples containing pNP-Man and CelB R77Q or CelB R77Q/N206D after prolonged incubation at 90 °C (data not shown). Previously, oligosacharide synthesis by CelB from pentose substrates has been described (*32*). Although the β-mannosidase activity was increased relative to the β-glucosidase and β-galactosidase activity, β-glucosidase activity was still the most dominant activity in all CelB

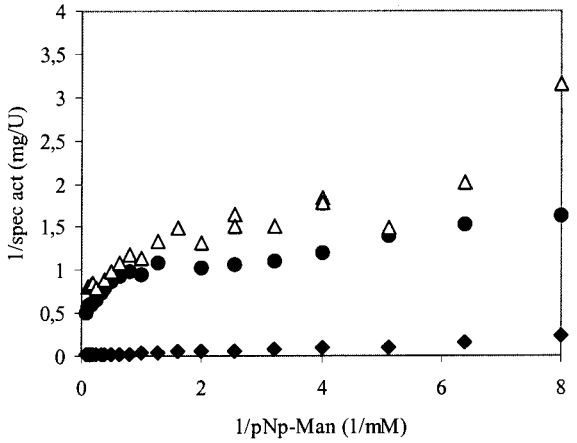

FIGURE 4: Lineweaver-Burk plot for the hydrolysis of pNP-Man at 90 °C by wild-type CelB (◆), CelB R77Q (△), and CelB R77Q/N206D (●).

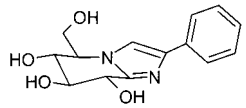

FIGURE 5: Molecular structure of the thermostable transition-state inhibitor PheImGlc.

mutants. This indicates that besides the unique active site residues, the position of the other conserved active site, or second-shell residues, contributes to the specificity differences between the two wild-type enzymes, similar to what has been found in earlier studies (*26*).

In BglB, the introduction of an arginine at position 77 (Q77R) and an asparagine at position 206 (D206N) has different effects (Table 1). When glutamine 77 was replaced by an arginine, none of the catalytic parameters on all three substrates was improved. However, upon the introduction of D206N, the k_{cat} on all substrates increased about 10-fold, and the K_m for the hydrolysis of pNP-Glc was reduced 45-fold. This made BglB D206N effectively a β-glucosidase. As in the CelB double mutant, BglB Q77R/D206N showed the combined characteristics of the respective single mutants. These results show that the differences in activity between CelB and BglB are the result of their active site composition. As retaining enzymes, the hydrolysis of saccharides by BglB and CelB occurs by formation of a glycosyl-enzyme intermediate in which the glycosidic bond is hydrolyzed. Next, the glycosyl-enzyme bond is hydrolyzed. Since nitrophenol is an excellent leaving group, the parameters obtained in this study provide information about the latter, deglycosylating step of the reaction (*8*), as previously was demonstrated for wild-type CelB (*32*). However, this has not been verified for wild-type BglB or the BglB and CelB mutants.

Inhibition of Mutant and Wild-Type Enzymes by PheImGlc. Many glucose derivatives with a more or less trigonal C1 atom, such as glucono-lactone, inhibit family 1 glycoside hydrolases, but are insufficiently stable under hydrolytic or thermal conditions to be suitable for inhibition experiments at elevated temperatures. The inhibitor PheImGlc has a trigonal geometry at the center corresponding to C1 and is thermostable, as expected on the basis of the aromatic character of the imidazole ring (Figure 5). PheImGlc was used to test the inhibition of pNP-Glc hydrolysis at 90 °C by CelB, BglB, and mutants (Tables 1 and 2). At this temperature, the inhibitor PheImGlc was stable within the

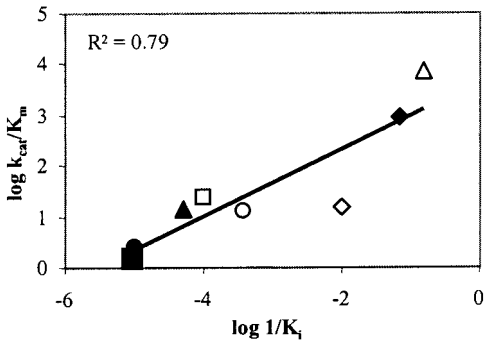

FIGURE 6: Correlation of activation free energy for turnover of pNP-Glc [log (k_{cat}/K_m)] by the CelB and BglB variants with the corresponding free energy of binding of the transition-state analogue PheImGlc [log ($1/K_i$)]. CelB wt (△), CelB R77Q (◇), CelB N206D (□), CelB R77Q/N206D (○), BglB wt (●), BglB Q77R (■), BglB D206N (◆), BglB Q77R/D206N (▲).

time span of an activity assay (6 min). All enzymes were inhibited competitively by PheImGlc, although there were large differences in sensitivity toward the thermostable inhibitor. The inhibition constant of CelB for PheImGlc was found to be 6.5 nM. This value is lower than found with PheImGlc for the β-glucosidases from almond (100 nM) and *Caldocellum saccharolyticum* (18 nM) (*14*). Assuming, by analogy (*53*), that this inhibitor is at least a partial transition-state analogue, this means that the active site of CelB (at 90 °C) is slightly more adapted to stabilize the reaction transition state than the β-glucosidases of almond and *C. saccharolyticum*. Also, the reported inhibitor constant for the transition-state analogue glucono-lactone for pNP-Glc hydrolysis by CelB was over 1000-fold higher than for PheImGlc (*32*). The PheImGlc inhibition constant for mutant CelB R77Q was 15-fold higher than for the wild-type enzyme, but was still relatively low compared to the 1500-fold increase of the inhibition constant for CelB N206D. The CelB double mutant was slightly more sensitive to inhibition by PheImGlc than CelB N206D. Wild-type BglB was 15 000-fold less strongly inhibited by PheImGlc than wild-type CelB. BglB Q77R displayed a similar sensitivity. Strikingly, the inhibition constant for BglB D206N was comparable to that of CelB wild-type. The BglB double mutant was slightly more sensitive than wild-type BglB and BglB Q77R.

Conceivably, differences in accommodating the phenyl substituent of the inhibitor between the mutants may also contribute to differences in the inhibition. However, this option is not supported by the observed correlation of log (k_{cat}/K_m) and log ($1/K_i$) for PheImGlc for the enzyme variants, which visualized a linear trend ($R^2 = 0.79$) between the free energy for activation and the binding energy for PheImGlc (Figure 6). This indicates that the mutated residues are directly involved in the stabilization of the transition states. Since the interaction of family 1 glycoside hydrolases with equatorial C2-hydroxyls of glucose is highly stabilizing in hydrolysis of the glycosidic bond (*19, 51*), these findings support the proposed involvement of the replaced residues in this interaction.

CONCLUSIONS

The pyrococcal β-mannosidase BglB and β-glucosidase CelB represent two different classes of family 1 glycoside hydrolases. Whereas CelB has been optimized for high-turnover saccharide hydrolysis, BglB is adapted for the specific, low rate catalysis of mannoside conversion. This specificity results directly from the unique active site residues as demonstrated by exchanging these residues with those present in the β-glucosidase CelB of *P. furiosus*. We have shown that in *P. furiosus* CelB the affinity for mannosides was increased at the cost of the turnover rate, while *P. horikoshii* BglB could be turned into an efficient β-glucosidase. An altered interaction between the glycoside 2-hydroxyl and the enzyme upon substrate binding could explain the differences in activity between these two enzymes. This study confirms the importance of the interaction between the C2-hydroxyl of the substrate and the enzyme during catalysis in family 1 glycoside hydrolases.

ACKNOWLEDGMENT

We thank Dr. Peter Barneveld (Wageningen University, Wageningen, The Netherlands) for assistance with the DSC analysis and Willy van den Berg (Wageningen University, Wageningen, The Netherlands) for help with the detection of oligosaccharides.

REFERENCES

1. Coutinho, P. M., and Henrissat, B. (1999) in *Recent Advances in Carbohydrate Bioengineering* (Gilbert, H. J., Davies, G., Henrissat, B., and Svensson, B., Eds.) pp 3−12, The Royal Society of Chemistry, Cambridge, U.K.
2. Vetter, J. (2000) *Toxicon 38*, 11−36.
3. Rask, L., Andreasson, E., Ekbom, B., Eriksson, S., Pontoppidan, B., and Meijer, J. (2000) *Plant Mol. Biol. 42*, 93−113.
4. Voorhorst, W., Gueguen, Y., Geerling, A., Schut, G., Dahlke, I., Thomm, M., Van der Oost, J., and De Vos, W. (1999) *J. Bacteriol. 181*, 3777−3783.
5. de Vos, W. M., Boerrigter, I., van Rooyen, R. J., Reiche, B., and Hengstenberg, W. (1990) *J. Biol. Chem. 265*, 22554−22560.
6. Fernandez, P., Canada, F. J., Jiminez-Barbero, J., and Martin-Lomas, M. (1995) *Carbohydr. Res. 271*, 31−42.
7. Bauer, M. W., Bylina, E. J., Swanson, R. V., and Kelly, R. M. (1996) *J. Biol. Chem. 271*, 23749−23755.
8. Kempton, J. B., and Withers, S. G. (1992) *Biochemistry 31*, 9961−9969.
9. White, A., and Rose, D. R. (1997) *Curr. Opin. Struct. Biol. 7*, 645−651.
10. Burmeister, W. P., Cottaz, S., Driguez, H., Iori, R., Palmieri, S., and Henrissat, B. (1997) *Structure 5*, 663−675.
11. Sidhu, G., Withers, S. G., Nguyen, N. T., McIntosh, L. P., Ziser, L., and Brayer, G. D. (1999) *Biochemistry 38*, 5346−5354.
12. Sanz-Aparicio, J., Gonzalez, B., Hermoso, J. A., Polaina, J., Arribas, J. C., and Canada, J. (2001) in preparation.
13. Notenboom, V., Birsan, C., Nitz, M., Rose, D. R., Warren, R. A. J., and Withers, S. G. (1998) *Nat. Struct. Biol. 5*, 812−818.
14. Panday, N., Canac, Y., and Vasella, A. (2000) *Helv. Chim. Acta 83*, 58−79.
15. Voorhorst, W. G., Eggen, R. I., Luesink, E. J., and de Vos, W. M. (1995) *J. Bacteriol. 177*, 7105−7111.
16. Wang, Q., Trimbur, D., Graham, R., Warren, R. A., and Withers, S. G. (1995) *Biochemistry 34*, 14554−14562.
17. Moracci, M., Capalbo, L., Ciaramella, M., and Rossi, M. (1996) *Protein Eng. 9*, 1191−1195.
18. McIntosh, L. P., Hand, G., Johnson, P. E., Joshi, M. D., Korner, M., Plesniak, L. A., Ziser, L., Wakarchuk, W. W., and Withers, S. G. (1996) *Biochemistry 35*, 9958−9966.
19. Namchuk, M. N., and Withers, S. G. (1995) *Biochemistry 34*, 16194−16202.

20. Rivera-Sagredo, A., Canada, F. J., Nieto, O., Jimenez-Barbero, J., and Martin-Lomas, M. (1992) *Eur. J. Biochem. 209*, 415−422.
21. Barrett, T., Suresh, C. G., Tolley, S. P., Dodson, E. J., and Hughes, M. A. (1995) *Structure 3*, 951−960.
22. Wiesmann, C., Beste, G., Hengstenberg, W., and Schulz, G. E. (1995) *Structure 3*, 961−968.
23. Sanz Aparicio, J., Hermoso, J. A., Martinez Ripoll, M., Lequerica, J. L., and Polaina, J. (1998) *J. Mol. Biol. 275*, 491−502.
24. Aguilar, C. F., Sanderson, I., Moracci, M., Ciaramella, M., Nucci, R., Rossi, M., and Pearl, L. H. (1997) *J. Mol. Biol. 271*, 789−802.
25. Chi, Y. I., Martinez-Cruz, L. A., Jancarik, J., Swanson, R. V., Robertson, D. E., and Kim, S. H. (1999) *FEBS Lett. 445*, 375−383.
26. Kaper, T., Lebbink, J. H. G., Pouwels, J., Kopp, J., Schulz, G. E., Van der Oost, J., and De Vos, W. M. (2000) *Biochemistry 39*, 4963−4970.
27. Hakulinen, N., Paavilainen, S., Korpela, T., and J., R. (2000) *J. Struct. Biol. 129*, 69−79.
28. Czjzek, M., Cicek, M., Zamboni, V., Burmeister, W. P., Bevan, D. R., Henrissat, B., and Esen, A. (2001) *Biochem. J. 354*, 37−46.
29. Wiesmann, C., Hengstenberg, W., and Schulz, G. E. (1997) *J. Mol. Biol. 269*, 851−860.
30. Kengen, S. W., Luesink, E. J., Stams, A. J., and Zehnder, A. J. (1993) *Eur. J. Biochem. 213*, 305−312.
31. Gueguen, Y., Voorhorst, W. G., van der Oost, J., and de Vos, W. M. (1997) *J. Biol. Chem. 272*, 31258−31264.
32. Bauer, M. W., and Kelly, R. M. (1998) *Biochemistry 37*, 17170−17178.
33. Kawarabayasi, Y., Sawada, M., Horikawa, H., Haikawa, Y., Hino, Y., Yamamoto, S., Sekine, M., Baba, S., Kosugi, H., Hosoyama, A., Nagai, Y., Sakai, M., Ogura, K., Otsuka, R., Nakazawa, H., Takamiya, M., Ohfuku, Y., Funahashi, T., Tanaka, T., Kudoh, Y., Yamazaki, J., Kushida, N., Oguchi, A., Aoki, K., and Kikuchi, H. (1998) *DNA Res. 5*, 147−155.
34. Kawarabayasi, Y. (2001) *Methods Enzymol. 330*, 124−134.
35. Matsui, I., Sakai, Y., Matsui, E., Kikuchi, H., Kawarabayasi, Y., and Honda, K. (2000) *FEBS Lett. 467*, 195−200.
36. Lebbink, J. H. G., Kaper, T., Kengen, S. W. M., Van der Oost, J., and De Vos, W. M. (2001) *Methods Enzymol. 330*, 364−379.
37. Guex, N., Diemand, A., and Peitsch, M. C. (1999) *Trends Biochem. Sci. 24*, 364−367.
38. Laskowski, R. A., MacArthur, M. W., Moss, D. S., and Thronton, J. M. (1993) *J. Appl. Crystallogr. 26*, 283−291.
39. Sippl, M. J. (1993) *Proteins: Struct., Funct., Genet. 17*, 355−362.
40. Higuchi, R., Krummel, B., and Saiki, R. K. (1988) *Nucleic Acids Res. 16*, 7351−7367.
41. Gill, S. C., and von Hippel, P. H. (1989) *Anal. Biochem. 182*, 319−326.
42. Kaper, T., Verhees, C. H., Lebbink, J. H. G., van Lieshout, J. F. T., Kluskens, L. D., Ward, D. E., Kengen, S. W. M., Beerthuyzen, M. M., de Vos, W. M., and van der Oost, J. (2001) *Methods Enzymol. 330*, 329−346.
43. Wong, J. T. (1977) *Kinetics of enzyme mechanisms*, 2nd ed., Academic press, London.
44. Cubellis, M. V., Rozzo, C., Montecucchi, P., and Rossi, M. (1990) *Gene 94*, 89−94.
45. Kengen, S., and Stams, A. (1994) *Biocatalysis 11*, 79−88.
46. Pisani, F. M., Rella, R., Raia, C. A., Rozzo, C., Nucci, R., Gambacorta, A., De Rosa, M., and Rossi, M. (1990) *Eur. J. Biochem. 187*, 321−328.
47. Lebbink, J. H. G. (1999) Ph.D. Thesis, Wageningen University, Wageningen, The Netherlands.
48. Moracci, M., Ciaramella, M., Cobucci-Ponzano, B., Perugino, G., Rossi, M. (1998) *International Conference on Thermophiles 1998*, Brest, France.
49. Sanchez, R., and Sali, A. (1998) *Proc. Natl. Acad. Sci. U.S.A. 95*, 13597−13602.
50. Davies, J. D., Mackenzie, L., Varrot, A., Dauter, M., Brzozowoski, A. M., Schülein, M., and Withers, S. G. (1998) *Biochemistry 37*, 11707−11713.
51. McCarter, J. D., Adam, M. J., and Withers, S. G. (1992) *Biochem. J. 286*, 721−727.
52. Joshi, M. D., Sidhu, G., Pot, I., Brayer, G. D., Withers, S. G., and McIntosh, L. P. (2000) *J. Mol. Biol. 299*, 255−279.
53. Ermert, P., Vasella, A., Weber, M., Rupitz, K., and Withers, S. G. (1993) *Carbohydr. Res. 250*, 113−128.
54. Thompson, J. D., Higgins, D. G., and Gibson, T. J. (1994) *Nucleic Acids Res. 22*, 4673−4680.
55. Page, R. D. C. (2000) Treeview 1.64b, Glasgow, U.K.
56. Guex, N., and Peitsch, M. C. (1997) *Electrophoresis 18*, 2714−2723.
57. Cason, C. (1999) The Persisitant of Vision Development Team, Indianapolis, IN.

BI011935A